A 4.5-mW 22-nm CMOS Label-Free Frequency-Shift 3 × 3 × 2 3-D Biosensor Array Using Vertically Stacked 60-GHz LC Oscillators

Akiyoshi Tanaka, *Graduate Student Member, IEEE*, Guowei Chen, *Graduate Student Member, IEEE*, and Kiichi Niitsu, *Member, IEEE*

***Abstract*—In this brief, a label-free 3 x 3 x 2 three-dimensional frequency-shift biosensor array with vertically-stacked 60-GHz on-chip LC oscillators is presented. The 60-GHz LC oscillators function as sensor front-end since the frequency downward shifts due to dielectric derived from biomedical sensing targets. The proposed array element consists of the two vertically-stacked LC oscillators and 15-stage dividers necessary for extracting high-frequency output signals with a long distance. The proposed circuit was designed with Spectre RF simulation and the test chip was fabricated in 22-nm CMOS technology. The whole and element chip size is 0.04 mm^2 and 0.0035 mm^2 respectively. The measurement with thick and thin silicon resin samples successfully demonstrated their vertical and horizontal detection on the same chip while the prior works only achieved two-dimensional detection. The 22-nm CMOS prototype also showed high spatial resolution 60μm x 60μm x 4μm and high fill factor 73% while consuming 4.5 mW under 1.2 V per the single-element.**

***Index Terms*—Biosensor, CMOS, LC oscillator, millimeter waves, biomedical measurements, point of care.**

I. Introduction

THESE days, many biomedical measurement devices have been proposed for realizing Point of Care testing systems. Among the biomedical measurement instruments, CMOS integrated circuit techniques are promising for fulfilling their requirements such as portable size, energy efficiency and cost performance with high accuracy. Above all, CMOS-based biosensor arrays [1]–[6] have shown the feasibility of overcoming those challenges in biomedical detection such as ion concentration, specific DNA sequences and aqueous solutions.

Manuscript received 11 April 2022; revised 11 June 2022; accepted 20 June 2022. Date of publication 22 June 2022; date of current version 26 September 2022. This work was supported in part by PRESTO/JST, Council for Science, Technology and Innovation (CSTI), Cross-Ministerial Strategic Innovation Promotion Program (SPI), "Energy Systems of an Internet of Energy (IoE) Society" (Funding Agency: JST) under Grant JPMJPR2034; in part by the Grant-in-Aid for Young Scientists (A) and Grant-in-Aid for Scientific Research (B) from MEXT of Japan under Grant 16H06088 and Grant 22H03557; and in part by MIC/SCOPE under Grant 152106004 and Grant 185106001 and NEDO Uncharted Territory Challenge 2050. This brief was recommended by Associate Editor S. Hoyos. *(Corresponding author: Kiichi Niitsu.)*

The authors are with the Department of Electronics, Nagoya University, Nagoya 464-8603, Japan (e-mail: niitsu@nuee.nagoya-u.ac.jp).

Color versions of one or more figures in this article are available at https://doi.org/10.1109/TCSII.2022.3185542.

Digital Object Identifier 10.1109/TCSII.2022.3185542

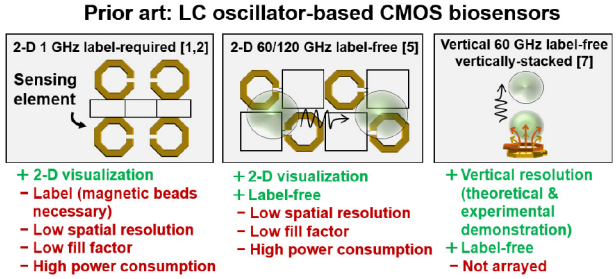

Fig. 1. The pros and cons in the recent prior art.

The frequency-shift biosensor arrays using CMOS LC oscillator-based approach were first proposed for detecting target molecules labeled by magnetic beads two-dimensionally (2D) [1], [2]. The latest work [6] extended them to ultra-low-power operation. The second generation of the frequency-shift 2D biosensor array [3], [4] demonstrated label-free detection with sub-10 GHz LC oscillators. The recent biosensor array introduced LC oscillators whose output is a millimeter-wave range and achieved high sensitivity and biomolecule detection without magnetically labeled targets [5].

While the LC-based frequency-shift detection schemes summarized in Fig. 1 have demonstrated the possibility for energy-efficient 2D detection with high fill factor or accuracy, they are unable to detect vertical biological phenomena such as diffusion migration and sedimentation of bio-organism or bio-molecules. For addressing this issue, [7] demonstrated the design and analysis of a frequency-shift biosensor that enabled vertical label-free detection with two vertically-stacked LC oscillators. However, the sensor cannot achieve horizontal detection at the same time since being not arrayed.

For three-dimensional (3D) detection on a single-biosensor array, a 3 × 3 × 2 3D biosensor array is proposed as shown in Fig. 2 which demonstrates label-free vertical and horizontal detection with 60-GHz LC oscillation. It also achieves high spatial resolution, high fill factor and low power operation [8].

This brief is an extended version of our conference contribution [8] and contains a more detailed explanation of the operational principle of LC oscillation as sensor front-end, new simulation results for more analysis and additional measurements using five test chips to evaluate the frequency variations and lower power consumption. The structure of this brief is

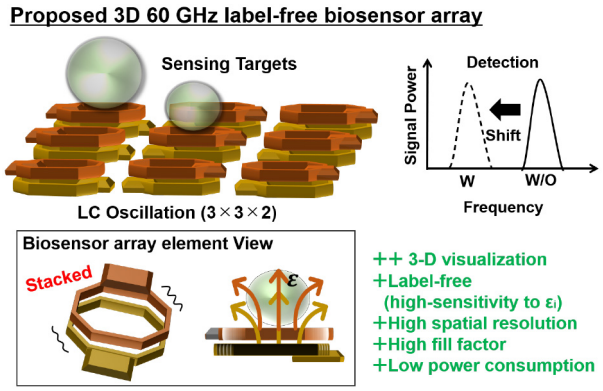

Fig. 2. Proposed work.

as follows: Section II explains the operational principle and structure of the proposed 3 × 3 × 2 3D biosensor array with simulation results. The chip measurements using five test chip in 22-nm CMOS and silicon resins are presented in Section III. In Section IV, we summarize this proposed work.

II. The Proposed 3D Biosensor Array

A. Operation Principle as Sensor Front-End

The two on-chip spiral inductors of LC oscillators in the proposed biosensor array take a role in its sensor front end by measuring the output frequency downward shifts. The output frequency of LC oscillators is generally defined as

$$f_0 = 1/(2\pi\sqrt{L_0C_0}) \tag{1}$$

where L_0 and C_0 mean designed inductance and capacitance size therein respectively.

As magnetic biosensor array, the output frequency of f_0 is down due to the inductance L increase caused by magnetic-labeled molecules [1]. Therefore, the inductance L_0 in (1) is replaced by $L = L_0 + \Delta L$ and the shifted oscillation frequency is determined as [2]

$$f \approx f_0\left(1 - \frac{\Delta L}{2L_0}\right) \tag{2}$$

In this brief, we used the 60-GHz LC oscillation since [5] explained frequency ranges from 50 to 100 GHz are reasonable for measuring the complex dielectric constant of aqueous solutions and [7] also showed 60 GHz is appropriate for biomolecules, biological cells and bacteria considering their frequency dependence of complex relative permittivity. The output frequency shifts in the label-free biosensor array including this brief is defined as [7]

$$f = 1/(2\pi\sqrt{L_0(C_0 + \Delta C)}) \tag{3}$$

ΔC is depended on dielectric constant (relative permittivity) of sensing targets. Reference [5] described ΔC more specifically as the function of both ε_r and ε_i;

$$\Delta C = \varepsilon_0 C' C_1 \frac{\varepsilon_r C_1 + \varepsilon_0 C'(\varepsilon_r^2 + \varepsilon_i^2)}{(C_1 + \varepsilon_0\varepsilon_r C')^2 + (\varepsilon_0\varepsilon_i C')^2} \tag{4}$$

where ε_0 is dielectric constant of vacuum, ε_r and ε_i is the real and imaginary part of complex dielectric constant derived from sensing targets. C_1 derived from the material existing between target and each inductor such as passivation. C' is derived from

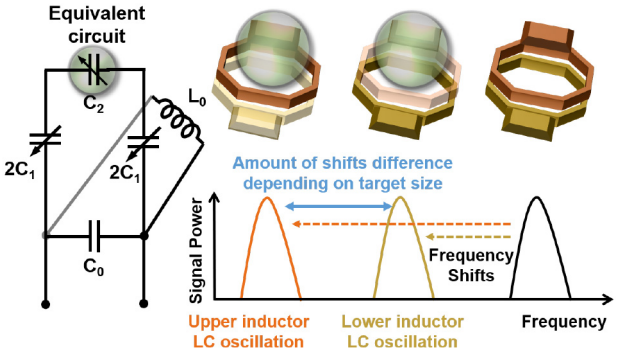

Fig. 3. Biomolecule detection with the proposed biosensor array.

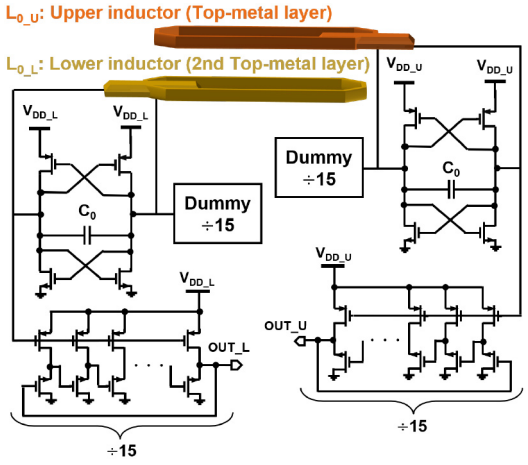

Fig. 4. Element schematic of the proposed 3D biosensor array.

the capacitance of the target $\varepsilon_r\varepsilon_0 C'(= C_2)$ and then constant. Since the complex dielectric constant is depended on the sort of targets, the amount of frequency shifts is reflected on it.

Fig. 3 shows the assumed vertical detection principle using the proposed 3 × 3 × 2 3D biosensor array and the equivalent circuit based on [5]. The frequency peak colored by black is in the state without any sensing targets, which corresponds to (1). The other frequency peak theoretically calculated by (3) and (4) shows the LC oscillation using the inductors on the top and second-top metal layers respectively when the target is placed over the array. While C_1 of (4) is constant in [5], C_1 is considered as a function of (4) in the case shown in Fig. 3 where the two different inductors on different metal layers when the same bio-material is placed over them. It means that ε_r and ε_i are unchanged. Thus, the difference between the amounts of the frequency shift implies distance from the upper and lower inductors.

B. Vertically-Stacked LC Oscillators-Based 3D Biosensor Array

A schematic of a single element in the proposed biosensor array is shown in Fig. 4. It is structured by two complementary LC oscillators and four 15-stages dividers. While the prior work using 65-nm CMOS [7] used NMOS-only LC oscillators from the viewpoint of chip size, Another work [9] reported that the NMOS-only LC oscillator was inferior to the complementary one in terms of noise phase and this introduction improves the noise. Therefore, this brief introduced the complementary

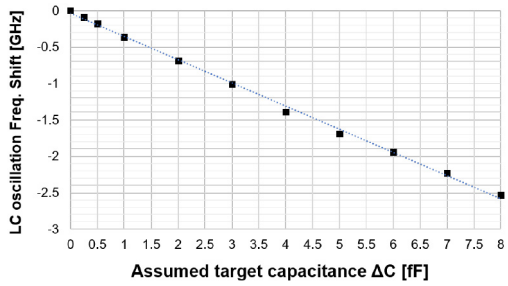

Fig. 5. Simulated frequency-shift in LC oscillation.

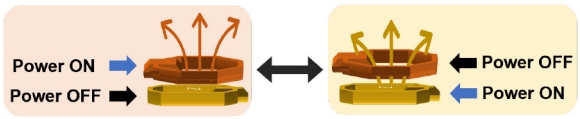

Fig. 6. Electrical isolation under measurement.

LC oscillators thanks to the 22-nm CMOS technology that helps reduce the area.

As for the 15-stages divider, the previous work [5] reported that the dividers are necessary for extracting high-frequency signal outputs from chips to peripherals with a long distance. We adopted a divide-by-3 frequency divider with three-phase harmonic injection locking [10] for this brief. The work [10] showed the maximum operating frequency was 6.0 GHz at first but [5] demonstrated its effectiveness for 60 GHz operation. The dividing ratio is 15. To make balance in terms of the load in the circuit, the dummy dividers that are identical dividing ratio should be designed on the other side.

In the chip design, two spiral inductors L_{0_U} and L_{0_L} are on the top and second-top metal layer and all the other components such as capacitors and transistors are on the rest of metal layers. The parameter of the inductors L_{0_U} and L_{0_L} are identical.

Fig. 5 shows simulated frequency-shift of the 60-GHz LC oscillator illustrated in Fig. 4 with Spectre RF. ΔC is a variable modeling the assumed capacitance of (4). From this result, linear correlation between the frequency shift and ΔC was confirmed, where the correlation coefficient was 0.9989. The simulation result also showed the relation was -0.318 [GHz/fF] and suggested the feasibility of the proposed biosensor array.

Note that supply voltage for the upper and the lower LC oscillator are switched alternately on and off as shown in Fig. 6 since electrical isolation should be kept between the two stacked oscillators. Also, only one sensing element is on and the other oscillators are off when measuring the frequency and its shifts. It is because crosstalk in the inductive coupling array is negligible, especially when using the time leaving technique [11]. Therefore, the degradation coming from the inductive-coupling can be negligible.

III. The 22-nm CMOS Chip Measurements

A. Test Chip Design and Measurement Setup

The chip prototype is implemented in 22-nm CMOS technology and its whole and element size is 0.04 mm^2 and 0.0035 mm^2 respectively. The on-chip spiral inductors L_{0_U} and L_{0_L} of 82 pH on top and second-top metal layers were designed and two metal-oxide-metal (MOM) capacitors C_0 of 35.6 fF for the on-chip LC oscillators were placed. These parameters including the transistor size were designed with Spectre RF.

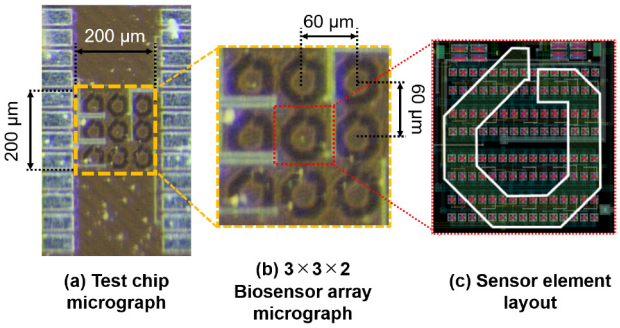

Fig. 7. (a) The microphotograph of 22-nm test chip, (b) The $3 \times 3 \times 2$ biosensor array photo, (c) The element of the proposed biosensor array layout image.

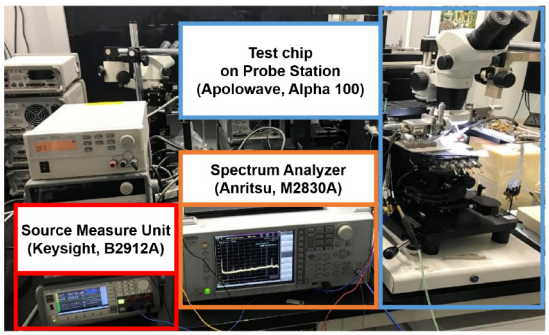

Fig. 8. Measurement setup.

The micrographs of the $3 \times 3 \times 2$ biosensor array and their element layout image are shown in Fig. 7. Considering the other circuit components could be mostly placed under the two inductors as the element image in Fig. 7 shows, we achieved the high spatial resolution and fill factor. The distance between each center of the inductors was 60 μm and that between two vertically-stacked inductors was sub-μm corresponding to a passivation layer thickness that determines vertical resolution. Thus, the resolution in the proposed work was $60 \times 60 \times 4 \mu m$ and the fill factor recorded 73%.

Fig. 8 shows the measurement setup, where the chip was placed on a manual probe station (Apolowave, Alpha 100) and the output frequency was measured with a spectrum analyzer (Anritsu, MS2830A). For a source measure unit, we used Keysight, B2912A.

B. Measurement Results

Chip verification was conducted to confirm the 60-GHz operation and the frequency variations due to the process and 3D biosensing scheme in the setup shown in Fig. 8. The measured frequency output from the proposed biosensor array on the spectrum analyzer is shown in Fig. 9. Since we employed a 15-stages local division in the biosensor array, the LC oscillator achieved the 60-GHz operation at the sensor front-end by capturing the 4-GHz output with the spectrum analyzer.

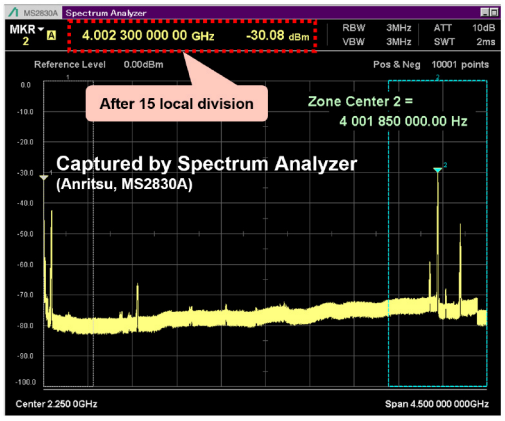

Fig. 9. Measured output frequency on the spectrum analyzer (M2830A).

The simulated phase noise of the upper 60 GHz LC oscillator was −79.993 [dBc/Hz] at 1 MHz offset from the central frequency with Spectre RF. The phase noise was a reasonable value, compared to the phase noise −100 [dBc/Hz] [12] and −86.4 [dBc/Hz] at 1 MHz offset [13] in the prior 60-GHz CMOS LC-Voltage-controlled oscillators. The measured Q value in the 4 GHz output that was divided from the upper 60 GHz LC oscillator was 75.16. The value should have improved thanks to the injection-locked divider [10] that we used. Power consumption was also measured with the source measure unit and the single element of the proposed biosensor array showed 4.5 mW under 1.2 V.

Fig. 10 shows the frequency measured from each embedded upper and lower LC oscillator of the five test chips at room temperature. The results vary from 3.955 GHz to 4.332 GHz and therefore the frequency on the sensor front-end ranges from 59.325 GHz to 64.98 GHz. In Fig. 10 (a), the normalized frequency measurement results are plotted at the target frequency of 4 GHz, where LC oscillation with the upper and lower inductors are plotted separately. The histogram of the original LC oscillation frequency is also illustrated in Fig. 10 (b). The average of the measured LC oscillation [μ] is 59.79 GHz. The standard deviation of the measurement [σ] is 0.854 GHz among the on-chip LC oscillation included in the five test chips and the coefficient of variation [σ/μ] is 1.43%, which we believe is at a level that is acceptable for practical use. Fig. 10 (c) shows the normalized frequency classified by the location. The output frequencies are within the 1.38 GHz range, except for the 3 LC oscillators. Comparing the process variation in Fig. 10 (b) and (c), even in the edge oscillators the variation is at the almost same level as in the center and middle oscillators. It means that the variation was mainly attributed to the process variation, not to the location.

For verifying the horizontal and vertical biomedical sensing, we used thick and thin silicon resins as the sample target in this work. Fig. 11 (a), (b) shows measured frequency shifts of the LC oscillators when the resins were directly placed over the prototype chip. The horizontal detection was seen by capturing the frequency shifts of the upper LC oscillators in each element as shown in Fig. 11 (a). The thick resin was on the left bottom of the biosensor array and the left corner

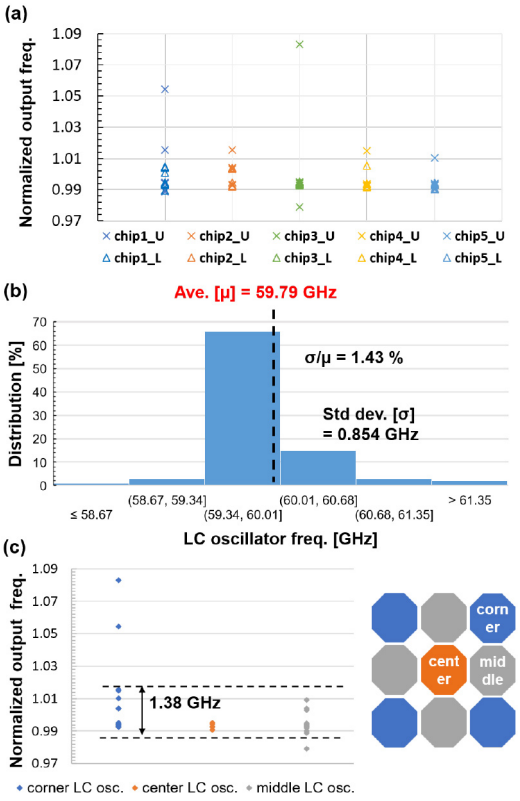

Fig. 10. (a) Measured LC oscillator frequency over the five test chips (b) Histogram of the measured LC oscillation frequency (c) Measured LC oscillator frequency classified by the location.

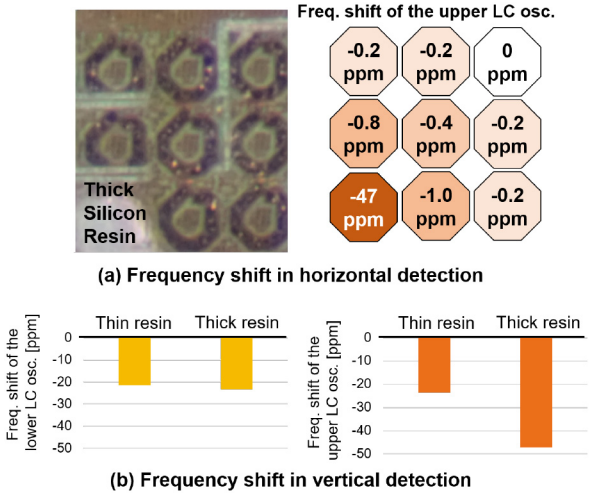

Fig. 11. (a) Measured frequency-shift of the upper LC oscillators in horizontal detection with thick resin (b) Measured frequency-shift difference in vertical detection with thick and thin silicon resins.

sensor element demonstrated −47 ppm downward frequency shift with the upper LC oscillator. The other sensor elements also showed a smaller frequency shift and the shift amount gradually decreased as an element is away from the thick resin. Therefore, comparing the frequency shifts in the nine sensor element, horizontal detection was achieved.

Fig. 11 (b) shows the experiment results for vertical detection using the thick and thin silicon resins. The upper LC

TABLE I
COMPARISON RESULTS

	ISSCC'09 [1]	IMS'10 [2]	JSCC'12 [3]	JSCC'16 [4]	JSCC'16 [5]	JSCC'18 [6]	This work
Frequency [GHz]	1	1	7-9.5	6.5/11/ 17.5/30	60/120	1.4/3.6	60
Label for bio-sensing	Magnetic beads	Magnetic beads	**Label Free**	**Label Free**	**Label Free**	Magnetic beads	**Label Free**
Spatial resolution [μm]	N. A.	187 x 187 (2D)	N. A.	N. A.	250x250/160x160 @120/60GHz (2D)	N. A.	**60 x 60 x4 (3D)**
Element size [mm^2]	N. A.	0.022	0.0625	0.212 @6.5GHz	0.014/0.008 @120/60GHz	0.17	**0.0035**
Fill Factor [%]	N. A.	44	N. A.	N. A.	29@120GHz 36@60GHz	N. A.	**73**
Visualization	2D (4 x 2 x1)	2D (8 x 8 x1)	N. A. (1 x 1 x1)	N. A. (1 x 1 x1)	2D (12 x 16 x1)	2D (2 x 2 x1)	**3D (3 x 3 x2)**
Power per element [mW]	165	80	16.5	16.3	34.8/12.2 @120/60GHz	5	**4.5**
Process	130-nm CMOS	65-nm CMOS	90-nm CMOS	65-nm CMOS	65-nm CMOS	65-nm CMOS	**22-nm CMOS**

oscillator showed -47 ppm downward frequency shift with the thick resin while the lower LC oscillator was -23.3 ppm. Alternately, the thin resin was placed in the same position as the thick resin. In this measurement, the downward shift of the upper and lower LC oscillation were -23.6 and -21.2 ppm respectively. The frequency shift difference between the upper and lower LC oscillation was 23.7 ppm in the measurement using the thick resin and 2.4 ppm in that using the thin one. From this result, it can be said that vertical detection is feasible in comparison with the frequency shifts of the upper and lower LC oscillators. The 3D detection on the proposed $3 \times 3 \times 2$ frequency-shift biosensor array was demonstrated through the measurements.

A more complete system for the future improvement should include the compensation for the frequency drifts of each LC oscillator caused by non-idealizes. As was discussed in [6], the drift happens due to the asymmetrical layout. Still, the difference is sufficiently slight and it does not largely affect the bacteria colony detection as demonstrated in [5] and our measurement results with the resins. For enhancing the sensitivity, the symmetric layout should be employed as shown in [6] instead of the asymmetrical layout. We can also compensate for the sensitivity by pre-shipment testing and after-shipment calibration since the difference is not so large. The frequency drift may also be caused due to the environmental noise such as power supply noise and temperature. For tackling such environmental noises, in-situ thermal or supply noise measurements on the array using tiny sensors are effective as demonstrated in [14], [15].

Table. I shows the comparison of the proposed 3D CMOS biosensor array with the recent prior works in frequency-shift CMOS biosensor arrays. From Table I, this brief exhibits the label-free 3D bio-molecule detection with a single chip for the first time. Compared to [5], this brief improved spatial resolution 2.67$\times$ and increased fill factor by 37%. This brief demonstrated 0.0035 mm^2 element size, which is the smallest chip area. Also, 4.5 mW power operation under 1.2 V per single-sensing element is the lowest while [6] demonstrated 5 mW consumption per element. The 4.5 mW power consumption is low enough to suppress the chip temperature under operation.

IV. CONCLUSION

This brief demonstrated the design and experimental verification of the 3D frequency-shift fully-integrated biosensor array using vertically-stacked LC oscillators. By placing stacked LC oscillators over the other circuits, three-dimensional detection becomes feasible. The 0.04 mm^2 prototype biosensor array chip in 22-nm CMOS technology successfully showed its operation with 4.5 mW under 1.2V and demonstrated the horizontal and vertical detection with thick and thin silicon resin samples.

ACKNOWLEDGMENT

The fabrication of CMOS chip was supported by the VLSI Design and Education Center (VDEC), University of Tokyo in collaboration with Cadence Design Systems, Inc and Mentor Graphics Corporation.

REFERENCES

[1] H. Wang, Y. Chen, A. Hassibi, A. Scherer, and A. Hajimiri, "A frequency-shift CMOS magnetic biosensor array with single-bead sensitivity and no external magnet," in *IEEE Int. Solid-State Circuits Conf. Dig. Tech. Papers*, 2009, pp. 438–439.

[2] H. Wang, S. Kosai, C. Sideris, and A. Hajimiri, "An ultrasensitive CMOS magnetic biosensor array with correlated double counting noise suppression," in *Proc. IEEE MTT-S Int. Microw. Symp.*, 2010, pp. 616–619.

[3] A. A. Helmy *et al.*, "A self-sustained CMOS microwave chemical sensor using a frequency synthesizer," *IEEE J. Solid-State Circuits*, vol. 47, no. 10, pp. 2467–2483, Oct. 2012.

[4] J.-C. Chien and A. M. Niknejad, "Oscillator-based reactance sensors with injection locking for high-throughput flow cytometry using microwave dielectric spectroscopy," *IEEE J. Solid-State Circuits*, vol. 51, no. 2, pp. 457–472, Feb. 2016.

[5] T. Mitsunaka *et al.*, "CMOS biosensor IC focusing on dielectric relaxations of biological water with 120 and 60 GHz oscillator arrays," *IEEE J. Solid-State Circuits*, vol. 51, no. 11, pp. 2534–2544, Nov. 2016.

[6] C. Sideris, P. P. Khial, and A. Hajimiri, "Design and implementation of reference-free drift-cancelling CMOS magnetic sensors for Biosensing applications," *IEEE J. Solid-State Circuits*, vol. 53, no. 11, pp. 3065–3075, Nov. 2018.

[7] M. Matsunaga, T. Nakanishi, A. Kobayashi, K. Nakazato, and K. Niitsu, "Design and analysis of a three-dimensional millimeter-wave frequency-shift based CMOS biosensor using vertically stacked spiral inductors in LC oscillators," *Analog Integr. Circuits Signal Process.*, vol. 98, pp. 453–464, Mar. 2019. [Online]. Available: https://doi.org/10.1007/s10470-018-1267-5

[8] A. Tanaka, G. Chen, and K. Niitsu, "A 4.8mW 22nm CMOS fully-integrated 60-GHz $3 \times 3 \times 2$ 3D frequency-shift biosensor array using vertically-stacked LC oscillators," in *Proc. 28th IEEE Int. Conf. Electron., Circuits, Syst. (ICECS)*, 2021, pp. 1–4.

[9] A. Hajimiri and T. H. Lee, "Design issues in CMOS differential LC oscillators," *IEEE J. Solid-State Circuits*, vol. 34, no. 5, pp. 717–724, May 1999.

[10] M. Motoyoshi and M. Fujishima, "43μW 6GHz CMOS divide-by-3 frequency divider based on three-phase harmonic injection locking," in *Proc. IEEE Asian Solid-State Circuits Conf.*, 2006, pp. 183–186.

[11] N. Miura, T. Sakurai, and T. Kuroda, "Crosstalk countermeasures for high-density inductive-coupling channel array," *IEEE J. Solid-State Circuits*, vol. 42, no. 2, pp. 410–421, Feb. 2007.

[12] D. Huang *et al.*, "A 60GHz CMOS VCO using on-chip resonator with embedded artificial dielectric for size, loss and noise reduction," in *IEEE Int. Solid State Circuits Conf. Dig. Tech. Papers*, 2006, pp. 1218–1227.

[13] Z.-Y. Huang, "A 57.15–59.00GHz CMOS LC-VCO for V-band high speed WPAN communication system," in *Proc. 41st Eur. Microw. Conf.*, 2011, pp. 671–673.

[14] K. Luria and J. Shor, "Miniaturized CMOS thermal sensor array for temperature gradient measurement in microprocessors," in *Proc. IEEE Int. Symp. Circuits Syst.*, 2010, pp. 1855–1858.

[15] Y. Kanno *et al.*, "In-situ measurement of supply-noise maps with millivolt accuracy and nanosecond-order time resolution," *IEEE J. Solid-State Circuits*, vol. 42, no. 4, pp. 784–789, Apr. 2007.